Outer hair cell electro-mechanical power conversion

Richard D. Rabbitt
Biomedical Engineering, Otolaryngology, and Neuroscience Program
University of Utah
36 S. Wasatch Drive, SMBB 3100
Salt Lake City, UT 84112

Email: r.rabbitt@utah.edu
Ph: 1 801 581-6968

Figures	2
Citations	26

Words

121	Abstract
361	Introduction
1219	Theory / Methods
823	Results
701	Discussion

Outer hair cell electro-mechanical power conversion

Abstract

Outer hair cells are the cellular motors in the mammalian inner ear responsible for sensitive high-frequency hearing. Motor function requires expression of the protein prestin in the OHC lateral membrane and mechano-electrical transduction in the apical hair bundle. In the present report, electrical power consumption and mechanical power output are determined from previously published data from isolated OHCs and membrane patches. Results reveal that power output by the prestin-motor complex peaks at a best frequency much higher than implied by the low-pass character of nonlinear capacitance, and much higher than the whole-cell resistive-capacitive corner frequency. High frequency power output is enabled by a -90° shift in the phase of prestin-dependent electrical charge displacement, manifested electrically as emergence of imaginary-valued nonlinear capacitance.

Keywords: electromotility, prestin, cochlea, piezoelectricity, electro-mechanics, biological motor, imaginary capacitance

Introduction

Amplification of sound-induced vibrations in the cochlea is ultrafast and operates at frequencies at least two orders of magnitude higher than possible by conventional molecular motors that rely on step-by-step ATP hydrolysis (Lymn and Taylor 1971). The cochlea avoids the limiting speed of hydrolysis by drawing power from the standing endolymphatic potential (EP), an electrochemical battery that is maintained by the metabolically active stria vascularis (Koppl, Wilms et al. 2018). Electro-mechanical power conversion is carried out by outer hair cells (OHCs) (Brownell, Bader et al. 1985), which are responsible for dramatically increasing the magnitude of vibrations near the cochlear traveling wave peak (Cooper, Vavakou et al. 2018, Dewey, Applegate et al. 2019). OHC motor function is imparted by expression of the transmembrane protein prestin (Zheng, Shen et al. 2000, Liberman, Gao et al. 2002) through a mechanism that couples voltage-driven electrical charge displacement in the protein motor complex directly to changes in cell length. Electro-mechanical coupling works in reciprocal directions (Dong, Ospeck et al. 2002), rendering the OHC lateral wall membrane piezoelectric on the continuum level (Mountain and Hubbard 1994, Tolomeo and Steele 1995). Structural evidence suggests piezoelectricity arises from conformational changes in prestin dimers along with concomitant changes in electrical charge displacement and membrane area occupied by the protein complex (Bavi, Clark et al. 2021, Ge, Elferich et al. 2021). Electro-mechanics of isolated OHCs (Frank, Hemmert et al. 1999) and measurements of vibrations in the living cochlea (Wang, Steele et al. 2016, Dewey, Altoe et al. 2021) provide strong evidence that OHC power output occurs cycle-by-cycle over the entire auditory frequency range. Amplification occurs even though nonlinear capacitance (NLC) (Gale and Ashmore 1997, Santos-Sacchi and Tan 2019), distortion products (Vavakou, Cooper et al. 2019) and voltage (Housley and Ashmore 1992, Dallos and Evans 1995) all exhibit low-pass characteristics. Theoretical analysis of OHC biophysics suggests low-pass character of NLC occurs as the result of the cell transitioning from a state of inefficient electro-mechanical power conversion at low frequencies to a state of highly effective electro-mechanical power conversion at high frequencies (Rabbitt 2020). The present report confirms this theoretical prediction by directly determining the electrical power consumed and mechanical power output based on previously published experimental data.

Methods

Electrical Power Consumed. Methods for power analysis presented here are predicated on the hypothesis that the prestin-motor complex is powered entirely by EP driven mechano-electrical transduction (MET) current entering the cell, which is partially converted into mechanical

power output through voltage-driven electrical charge displacement q^p in the soma by the prestin-motor complex. The analysis is focused on the prestin somatic motor, and the contribution of MET-related bundle motility is not considered. To analyze electro-mechanical power conversion based on data, the OHC is treated as a single electrical compartment, where the voltage and current are related by Kirchhoff's law:

$$c^l \frac{dv}{dt} + \frac{dq^p}{dt} + i_i = i. \tag{1}$$

The transmembrane voltage is v, the input current is i and the total ionic channel current is i_i. The electrical displacement current in the passive membrane is $c^l \frac{dv}{dt}$, which acts in parallel with voltage driven electrical displacement currents driving OHC motor function, $\frac{dq^p}{dt}$. For small perturbations about a resting state, charge displacement in the prestin-motor complex is written: $\frac{dq^p}{dt} = c^s \frac{dx}{dt}$, where x is the somatic displacement arising from strain s (concomitant with conformational change) in the prestin-motor complex. The parameter c^s is the capacitance strain susceptibility and is a constant for small deformations. Electrical power is estimated in the frequency domain about a reference state (v_o, i_o, x_o). Linearizing and taking the Fourier transform of Eq. 1 gives:

$$C^L j\omega V + C^S j\omega X + I_i = I \tag{2}$$

where upper case denotes small perturbations the frequency domain, ω is frequency (rad-s^{-1}) and $j = \sqrt{-1}$. The coefficient $C^S = \frac{\partial Q}{\partial X}$ determines the electrical current driving the prestin-motor complex. I_i describes the linearized ionic currents in the frequency domain and consists of capacitive, conductive, and inductive components (e.g. (Sirovich and Knight 1977)). I is the input current *via* the MET channels or patch electrode.

Electrical power is determined by multiplying Eq. 2 by the complex conjugate of voltage (V^*) and taking half of the real part. The right-hand side gives the electrical power input P_E *via* the MET channels or patch electrode:

$$P_E = \frac{1}{2} Re(IV^*), \tag{3}$$

which is the *input electrical power* available from cycle-by-cycle modulation of the MET receptor current (or electrode current) and the voltage. The left-hand side gives the electrical power lost to ion-channels:

$$P_I = \frac{1}{2} Re(I_i V^*), \tag{4}$$

and the electrical power consumed by the prestin-motor complex:

$$P_P = \frac{-\omega C^S}{2} Im(XV^*). \tag{5}$$

Notably, the electrical power consumed by the motor complex is zero if the voltage is in phase with the displacement, and maximum if the voltage is in phase with velocity. A small fraction of the electrical power consumed by the motors is dissipated as heat while the remainder is delivered to the mechanical load. C^S varies with reference state (v_o, i_o, x_o), but is nearly constant for small sinusoidal perturbations in voltage, current and displacement about the reference state. Frequency and load dependence arise implicitly from the somatic displacement X. The coefficient C^S can be determined experimentally in the frequency domain after blocking ion channels. The direct approach is to measure V, I and X and apply Eq. 2 to estimate C^S.

For low frequency voltage clamp recordings from OHCs in the dish, voltage is in phase with displacement, and power conversion by the prestin-motor complex is zero (Eq. 5). Hence, low frequency electromotility is only indirectly related to OHC function as a motor. Significant power conversion only occurs at high frequencies as viscosity compels the cell displacement to shift ~90º relative to the voltage, maximizing P_P in Eq. 5.

Although simple, the form of Eq. 5 is difficult to use experimentally because it requires knowing C^S and measuring X and V at the same time. Experiments are simplified by considering the electrical and mechanical sides of the problem separately. Writing the OHC displacement as a function of voltage and force: $X = X(V, F)$ and expanding in a Taylor series gives the total capacitive current $j\omega C^S X = j\omega(C^V V + C^F F)$, where the capacitance voltage susceptibility is $C^V = C^S \frac{\partial X}{\partial V}$ and the capacitance force susceptibility is $C^F = C^S \frac{\partial X}{\partial F}$. After blocking ion channels, C^V can be measured in voltage clamp under constant force, and C^F can be measured in force clamp under constant voltage. While C^S is a constant independent of load, both C^V and C^F depend on

the mechanical strain in the prestin-motor complex and therefore depend on how the cell is loaded. Under ideal voltage clamp, a command voltage V causes the cell to displace against the load imposed by the cell itself and the environment (stiffness, viscosity, mass). When working against a load, the force is a frequency-dependent function of voltage (e.g. $F = TV$). Combining terms, the total capacitive current is $j\omega C^N V$ (where $C^N = C^V + TC^F$), and the power consumed by the prestin-motor complex is given by the simple expression (Rabbitt 2020):

$$P_P = \frac{-\omega}{2} Im(C^N)V^2, \tag{6}$$

where C^N is the traditional NLC recorded under voltage clamp. Application of Eq. 6 simply requires experimental measurement of C^N and V, and is a valid approximation regardless of the biophysical origin(s) of NLC. Eq. 6 clearly has experimental advantages over Eq. 5, but it's very important to recognize that C^N depends on how the cell or membrane patch is loaded, and therefore depends on the experimental conditions. It is obvious from Eq. 6, if C^N is real-valued there is no power conversion and no motor function. For the prestin-motor complex to work as an electro-mechanical motor, C^N must be imaginary-valued and negative. Experimental data demonstrate that negative $Im(C^N)$ indeed emerges at high frequencies in OHCs and prestin expressing membrane patches as $Re(C^N) \to 0$ (Farrell, Ugrinov et al. 2006, Santos-Sacchi, Navaratnam et al. 2021).

Mechanical Power Output. In the frequency domain, mechanical power output by the prestin-motor complex is:

$$P_{PM} = \frac{-\omega}{2} Im(XF^*), \tag{7}$$

where X is the axial cell displacement and F is the axial somatic force. Eq. 7 can be used to estimate power output irrespective of the biophysical origins of force, but it is informative to demonstrate how it is related to electrical power consumed if the prestin-motor complex is an ideal piezoelectric. For a simple 1D homogeneous piezoelectric model the force is related to the displacement and the voltage by $F = \frac{1}{\kappa\ell}X + \frac{\delta}{\kappa}V$, where κ is the compliance, ℓ is the cell length, δ is the piezoelectric strain coefficient and $X = S\ell$ is the whole cell axial displacement arising from strain S. Substituting into Eq. 7 gives the piezoelectric prediction for mechanical power output:

$$P_{PM} \approx \frac{-\delta\omega}{2\kappa} Im(XV^*), \tag{8}$$

where the stiffness term is conservative and results in zero power. Eq. 8 was derived from mechanical power, but is identical to Eq. 5 derived from electrical power providing $C^S = \frac{\delta}{\kappa}$ (piezoelectric force coefficient). Hence, in the simple piezoelectric model, electrical power consumed by prestin is equal to the mechanical power driving displacement of the molecular motor complex, the cell and the extrinsic load – as required based on the second law of thermodynamics.

Mechanical Power Dissipated by the Load. Power consumed by the prestin-motor complex is partially dissipated by heat in the cell itself and partially transmitted to the extrinsic mechanical load -- a load that varies systematically in the cochlea along the tonotopic map. Insight can be gained into OHC power output by my treating the cochlear load as a simple spring-mass-damper. From Newton's 2nd law: $D^L X = F^T$, where the frequency domain operator D^L is

$$D^L = K^L \left(1 - \left(\frac{\omega}{\omega_0}\right)^2 + \zeta^L \left(\frac{j\omega}{\omega_0}\right)^n\right), \tag{8}$$

X is displacement of the load and F^T is the total force (OHC generated force plus applied force). Stiffness of the load is K^L, the natural frequency is ω_0 and the nondimensional viscous drag coefficient is ζ^L. Eq. 8 uses a fractional derivative n to model the viscous load (Rabbitt 2020), which gives rise to a power-law frequency dependence of *NLC* and electromotility approximating that recorded experimentally (Santos-Sacchi and Tan 2018). For an isolated cell in the dish, D^L describes intrinsic properties of the cell itself and the media, and in the cochlea D^L describes the addition of the intrinsic properties plus the cochlear load with frequency, stiffness and damping parameters adjusted accordingly. Multiplying Eq. 8 by velocity and integrating over time gives the power consumed by the viscous load in the frequency domain:

$$P_M = \frac{c\omega^{1+n}}{2} sin\left(\frac{n\pi}{2}\right) X^2. \tag{9}$$

where the damping parameter $c = \frac{K^L \zeta^L}{\omega_0^n}$, and n gives the power-law dependence of dissipation. For $n = 1$, Eq. 9 reduces to the well-known expression for power consumption by a viscous damper: $P_M = \frac{c\omega^2}{2} X^2$. As expected, mass and stiffness do not appear in Eq. 9. Total mechanical power output can easily be estimated from Eq. 9 based on whole-cell displacement in the frequency domain after estimating the viscous dissipation parameters c and n.

Results

Mechanical Power Output Delivered to the Dissipative Load. To determine frequency dependence of OHC motor function in isolated cells, mechanical power output was determined from high-frequency displacement data reported by Frank et al. (1999) (Frank, Hemmert et al. 1999) and Santos-Sacchi and Tan (2018) (Santos-Sacchi and Tan 2018). The procedure requires first estimating the viscous dissipation coefficient and power-law exponent, and then applying Eq. 9 to calculate the power output. Parameters were estimated from the frequency dependence of whole-cell displacement and phase driven by extracellular voltage V_e applied to the base of OHCs in a μ-chamber (large pipette) configuration. Fig. 1A illustrates the μ-chamber recording set up, the displacement magnitude (2B) and phase (2C), recorded in response to sinusoidal voltage commands for four OHCs. Solid curves are fits to an overdamped spring-mass-damper (Eq. 8). The Frank et al. (1999) data were fit using frequency: $\omega_o = (3.45x10^5, 1.73x10^5)$ rad-s^{-1}, damping coefficient: $\zeta^L = (1.43,1.74)$ and exponent: $n = (0.84,0.90)$. The Santos-Sacchi & Tan data were fit using frequency: $\omega_o = (1.00x10^5, 0.61x10^5)$ rad-s^{-1}, damping coefficient: $\zeta^L = (3.21,4.14)$ and exponent $n = (0.65,0.60)$. The mechanical power output for each cell is shown in Fig. 1D. Using conventional damping $n = 1$ reduces goodness of the curve fits, but does not change conclusions regarding high-frequency power output. The isometric force generated in the μ-chamber configuration (~0.03 nN-mV^{-1} (Frank, Hemmert et al. 1999)) is smaller than in whole-cell voltage clamp (~0.10 nN-mV^{-1} (Iwasa and Adachi 1997)), so the power output would be higher under ideal voltage clamp compared to the extracellular voltage commands in the μ-chamber. Nevertheless, the μ-chamber data clearly show OHCs are capable of outputting substantial power at ultrasonic frequencies, peaking between 30 kHz and 74 kHz for the cells in Fig. 2D. OHC power output is maximum when the displacement of the cell lags the stimulus voltage by ~90º. We know from simple mechanical systems that power consumption by the viscous load is maximum when velocity is in phase with the force. Isometric force data reported by Frank et al. (1999) (Fig. 4 in (Frank, Hemmert et al. 1999)) indicate the force generated by voltage is nearly instantaneous. Results in Fig. 1 are consistent with this observation and suggest the frequency limit of OHC

power output is not the speed of force generation in the prestin-motor complex, but instead the speed is limited by the ability of the force to displace the load – a load in the μ-chamber arising from the media and the cell itself. The frequency of maximum power output is aligned with the damped natural frequency of the total load, and power output at high frequencies is ultimately limited by the mass of the total load. In the cochlea, the load varies along the tonotopic axis and arises from mechanical properties of the cochlear partition, fluids and OHCs themselves.

Electrical Power Converted by the Prestin-Motor Complex P_P. To determine the speed of the prestin-motor function in membrane patches, frequency-dependent electrical power consumption was determined directly from macro-patch NLC data reported and by Santos-Sacchi et al. (Santos-Sacchi, Navaratnam et al. 2021) and estimated from data reported by by Gale & Ashmore (Gale and Ashmore 1997). The experimental approach used by Gale and Ashmore measured $Re(C^N)$ (Fig. 1A, blue symbols, right axes), while Santos-Sacchi et al. measured both $Re(C^N)$ and $Im(C^N)$ (Fig. 1A B, solid black curves, left axes). The magnitude of the NLC differs between the two reports primarily due to the size of the patch. Both data sets clearly show $Re(C^N)$ declining with frequency (1A). $Re(C^N)$ has a low-pass characteristic beginning to roll off below 2kHz and showing a power-law frequency dependence. But, as shown above, the real component of NLC is not related to electro-mechanical power conversion and therefore has little to do with function of the prestin-motor complex as a motor. Instead, the electrical power consumed by the prestin-motor complex is equal to $-\omega\, Im(C^N)V^2/2$ (Eq. 6). The Santos-Sacchi et al. data clearly show $Im(C^N)$ is indeed negative and continues to increase in magnitude up to the highest frequency tested (Fig. 2B, solid black). The electrical power consumed during the Santos-Sacchi et al. experiments is shown in Fig. 2C (solid black), and continues to increase up to the highest frequency tested. To estimate power output in the Gale & Ashmore experiments, $Re(C^N)$ was used to determine the corresponding $Im(C^N)$ component (2B, blue), which was accomplished by assuming the macro-patch was working against a visco-elastic load described by Eq. 8. Curve fitting the frequency dependence of $Re(C^N)$ (2A, blue) provided the frequency dependence of $Im(C^N)$ (2B, blue). Eq. 6 was then used to estimate the frequency dependent power consumed by the prestin-motor complex in the Gale & Ashmore macro-patch experiments (2C, blue, $\omega_o = 1.26x10^5$ rad-s^{-1}, $\zeta^L = 1.5$, $n = 0.7$). Frequency-dependence of the power consumption estimated from the Gale & Ashmore experiments is remarkably similar to that determined directly from the Santos-Sacchi et al. data (compare 2C, thick black vs. thin blue). The peak power consumption is estimated to occur in the macro-patch configuration near 37 kHz, which is more than an order of magnitude higher than the NLC corner frequency in the same

experiments. By conservation of energy, the power consumed by the motor (2C) must be delivered to dissipation inside the cell itself and to viscosity of the extracellular fluid media. The magnitude of the power output is expected to change with membrane potential, as illustrated in Fig. 2D based on a simple piezoelectric model of a fluid-loaded membrane patch (Rabbitt 2020).

Discussion

Speed of the prestin-motor complex. Present results are consistent with the hypothesis that the speed of force generation by the prestin-motor complex is nearly instantaneous while the speed of conformational change is limited by the load acting on the protein complex. The load varies substantially between experimental conditions (e.g. isolated cell, membrane patch, in vivo). Simple power analysis of published data (Fig. 1-2) provides evidence that OHCs indeed output cycle-by-cycle power across the frequency range of mammalian hearing.

The present analysis shows the timing of prestin-motor charge displacement during the power stroke is shifted -90º relative to the charge displacement in the passive membrane capacitance. This phase shift is undeniably required for power output (Eq. 6 and Fig. 2), irrespective of molecular origins. The phase shift is reflected on the mechanical side as well. Mechanical power output to a dissipative viscous load requires force to be in phase with velocity (Eq. 9 and Fig. 1), which is consistent with voltage occurring in phase with displacement current in the prestin-motor complex. Membrane conductance contributes to electrical power loss (Eq. 4), while passive membrane capacitance and conductance are both expected to contribute to electro-mechanical impedance matching of the OHC to the cochlear load. Results further indicate that MET receptor power is sufficient to drive high-frequency mechanical power output, and that cycle-by-cycle modulation of the extracellular voltage is not required.

In summary, electro-mechanical power conversion requires negative $Im(C^N)$, which emerges only at high frequencies as $Re(C^N)$ becomes small. Although peak $Im(C^N)$ is smaller than peak $Re(C^N)$ resulting in a frequency dependent decline in the magnitude $Abs(C^N)$, the decline does not reflect the speed of the motor or a decline in electro-mechanical power conversion. Emergence of $Im(C^N)$ under voltage clamp conditions reveals a shift in the phase of the prestin-dependent charge displacement, which is in phase with dv/dt at low frequencies (giving rise to real NLC) and in phase with v at high frequencies where maximum power conversion occurs (giving rise to imaginary NLC). The phase shift is required to align force with velocity, which is requisite for OHCs in the cochlea to deliver the power necessary to overcome the viscous load.

Acknowledgement

Support was provided by the National Institutes on Deafness and other Communication Disorders grant R01 DC006685.

Figure Captions

Fig. 1. OHC mechanical power output. A). μ-chamber used to apply sinusoidal voltages with the OHC partially extending into media. B-C) Magnitude and phase of the displacement X measured by Frank et al. (Frank, Hemmert et al. 1999) and Santos-Sacchi & Tan (Santos-Sacchi and Tan 2018). Solid curves are curve-fits to Eq. 8 used to estimate the dissipation parameters "c" and "n" . D) Mechanical power output was determined from Eq. 9 and measured displacement X. Power output computed from the data peaked between 20 kHz and 74 kHz, when the phase of the displacement was -90º relative to the peak sinusoidal voltage.

Fig. 2. Membrane patch electrical power consumption. A) Real NLC, $Re(C^V)$, recorded from OHC membrane macro-patches reported by Gale & Ashmore (blue symbols) (Gale and Ashmore 1997) and by Santos-Sacchi et al. (thick black) (Santos-Sacchi, Navaratnam et al. 2021). B) Imaginary NLC , $Im(C^V)$, recorded from OHC membrane macro-patches reported by Santos-Sacchi et al. (thick black). C) Electrical power consumed by the prestin-motor complex computed using Eq. 6 from $Im(C^V)$ reported by Santos-Sacchi et al. (thick black), and estimated (see text) from the Gale & Ashmore data (thin blue lines). D) Voltage and frequency dependence of NLC corresponding to the solid curves (blue) in panels A-C.

Citations

Bavi, N., M. D. Clark, G. F. Contreras, R. Shen, B. G. Reddy, W. Milewski and E. Perozo (2021). "Prestin's conformational cycle underlies outer hair cell electromotility." Nature.

Brownell, W. E., C. R. Bader, D. Bertrand and Y. de Ribaupierre (1985). "Evoked mechanical responses of isolated cochlear outer hair cells." Science **227**(4683): 194-196.

Cooper, N. P., A. Vavakou and M. van der Heijden (2018). "Vibration hotspots reveal longitudinal funneling of sound-evoked motion in the mammalian cochlea." Nat Commun **9**(1): 3054.

Dallos, P. and B. N. Evans (1995). "High-frequency motility of outer hair cells and the cochlear amplifier." Science **267**(5206): 2006-2009.

Dewey, J. B., A. Altoe, C. A. Shera, B. E. Applegate and J. S. Oghalai (2021). "Cochlear outer hair cell electromotility enhances organ of Corti motion on a cycle-by-cycle basis at high frequencies in vivo." Proc Natl Acad Sci U S A **118**(43).

Dewey, J. B., B. E. Applegate and J. S. Oghalai (2019). "Amplification and Suppression of Traveling Waves along the Mouse Organ of Corti: Evidence for Spatial Variation in the Longitudinal Coupling of Outer Hair Cell-Generated Forces." J Neurosci **39**(10): 1805-1816.

Dong, X. X., M. Ospeck and K. H. Iwasa (2002). "Piezoelectric reciprocal relationship of the membrane motor in the cochlear outer hair cell." Biophys J **82**(3): 1254-1259.

Farrell, B., R. Ugrinov and W. Brownell (2006). Frequency dependence of admittance and conductance of the outer hair cell. Auditory Mechanisms, Processes and Models. A. Nuttall, T. Ren, K. Gillespie, K. Grosh and E. de Boer. New Jersey, World Scientific**:** 231-232.

Frank, G., W. Hemmert and A. W. Gummer (1999). "Limiting dynamics of high-frequency electromechanical transduction of outer hair cells." Proc Natl Acad Sci U S A **96**(8): 4420-4425.

Gale, J. E. and J. F. Ashmore (1997). "The outer hair cell motor in membrane patches." Pflugers Arch **434**(3): 267-271.

Ge, J., J. Elferich, S. Dehghani-Ghahnaviyeh, Z. Zhao, M. Meadows, H. von Gersdorff, E. Tajkhorshid and E. Gouaux (2021). "Molecular mechanism of prestin electromotive signal amplification." Cell **184**(18): 4669-4679 e4613.

Housley, G. D. and J. F. Ashmore (1992). "Ionic currents of outer hair cells isolated from the guinea-pig cochlea." J Physiol **448**: 73-98.

Iwasa, K. H. and M. Adachi (1997). "Force generation in the outer hair cell of the cochlea." Biophys J **73**(1): 546-555.

Koppl, C., V. Wilms, I. J. Russell and H. G. Nothwang (2018). "Evolution of Endolymph Secretion and Endolymphatic Potential Generation in the Vertebrate Inner Ear." Brain Behav Evol **92**(1-2): 1-31.

Liberman, M. C., J. Gao, D. Z. He, X. Wu, S. Jia and J. Zuo (2002). "Prestin is required for electromotility of the outer hair cell and for the cochlear amplifier." Nature **419**(6904): 300-304.

Lymn, R. W. and E. W. Taylor (1971). "Mechanism of adenosine triphosphate hydrolysis by actomyosin." Biochemistry **10**(25): 4617-4624.

Mountain, D. C. and A. E. Hubbard (1994). "A piezoelectric model of outer hair cell function." J Acoust Soc Am **95**(1): 350-354.

Rabbitt, R. D. (2020). "The cochlear outer hair cell speed paradox." Proc Natl Acad Sci U S A.

Santos-Sacchi, J., D. Navaratnam and W. J. T. Tan (2021). "State dependent effects on the frequency response of prestin's real and imaginary components of nonlinear capacitance." Sci Rep **11**(1): 16149.

Santos-Sacchi, J. and W. Tan (2018). "The Frequency Response of Outer Hair Cell Voltage-Dependent Motility Is Limited by Kinetics of Prestin." J Neurosci **38**(24): 5495-5506.

Santos-Sacchi, J. and W. Tan (2019). "Voltage Does Not Drive Prestin (SLC26a5) Electro-Mechanical Activity at High Frequencies Where Cochlear Amplification Is Best." iScience **22**: 392-399.

Sirovich, L. and B. W. Knight (1977). "On subthreshold solutions of the Hodgkin-Huxley equations." Proc Natl Acad Sci U S A **74**(12): 5199-5202.

Tolomeo, J. A. and C. R. Steele (1995). "Orthotropic piezoelectric properties of the cochlear outer hair cell wall." J Acoust Soc Am **97**(5 Pt 1): 3006-3011.

Vavakou, A., N. P. Cooper and M. van der Heijden (2019). "The frequency limit of outer hair cell motility measured in vivo." Elife **8**.

Wang, Y., C. R. Steele and S. Puria (2016). "Cochlear Outer-Hair-Cell Power Generation and Viscous Fluid Loss." Sci Rep **6**: 19475.

Zheng, J., W. Shen, D. Z. He, K. B. Long, L. D. Madison and P. Dallos (2000). "Prestin is the motor protein of cochlear outer hair cells." Nature **405**(6783): 149-155.

Figure 1.

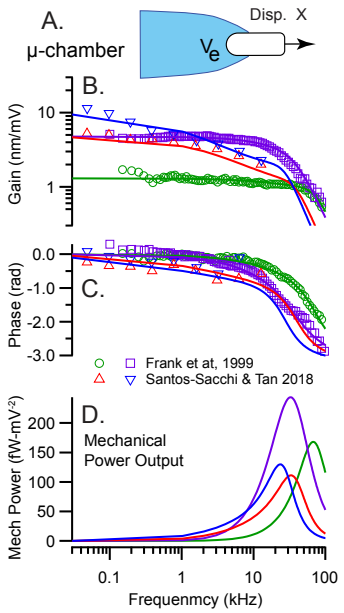
A.
μ-chamber
Disp. X
V_e
B.
Gain (nm/mV)
10
1
C.
Phase (rad)
0.0
-1.0
-2.0
-3.0
Frank et at, 1999
Santos-Sacchi & Tan 2018
D.
Mechanical
Power Output
Mech Power (fW-mV^{-2})
200
150
100
50
0
0.1
1
10
100
Frequenmcy (kHz)

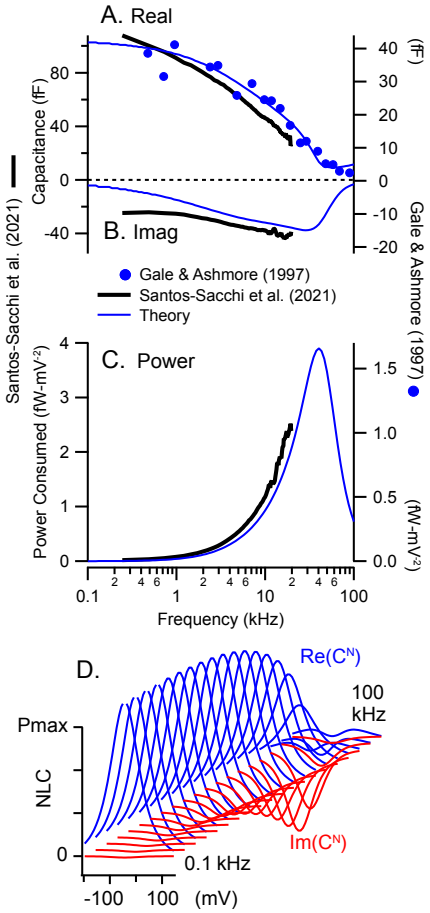
A. Real
B. Imag
Capacitance (fF)
Gale & Ashmore (1997)
Santos-Sacchi et al. (2021)
Theory
C. Power
Power Consumed (fW-mV⁻²)
Frequency (kHz)
D.
Pmax
NLC
Re(C^N)
Im(C^N)
100 kHz
0.1 kHz
-100
100
(mV)